Ab Initio Conformational Study of 1,2:4,5-Di-*O*-isopropylidene-*myo*-inositol

Sang Joo Lee, Seung Joo Cho, Kyung Seok Oh, Chunzhi Cui, Youngha Ryu, Young-Tae Chang, Kwang S. Kim,* and Sung-Kee Chung*

Department of Chemistry, Center for Biofunctional Molecules, Pohang University of Science and Technology, San 31, Hyojadong, Namgu, Pohang 790-784, Korea

Received: February 5, 1996; In Final Form: April 11, 1996[⊗]

Inositol phosphate derivatives play key roles in intracellular signal transduction. The X-ray structure of 1,2:4,5-diisopropylidene-*myo*-inositol is different from the conformer predicted by NMR and IR spectra. Therefore, we performed *ab initio* conformational study of the molecule, as a preliminary study before investigating the regioselectivity displayed by the *myo*-inositol toward electrophiles. The relative stabilities of four possible conformers of the molecule were investigated at various levels of *ab initio* theory: Hartree−Fock (HF) theory, Möller−Plesset second-order perturbation (MP2) theory, density functional theory (DFT), and self-consistent reaction field (SCRF) theory. Various basis sets were also tested. All calculations gave a consistent result which shows strong intramolecular hydrogen bonding interaction in an isolated system such as gas phase or solution. This is in agreement with NMR experiment. The frequency splitting between two OH vibrational frequencies due to the difference in the strength of the intramolecular hydrogen bonding is found to be very small (only several cm^{-1}) in contrast to a large frequency difference to appear in the intermolecular hydrogen bonding. On the other hand, in the solid phase, the intermolecular hydrogen bonding is expected to be important due to the crystal packing effect, as shown in the X-ray structure.

I. Introduction

Recent progress in understanding the intracellular signal transduction pathway utilizing inositol phosphate derivatives has stimulated the interest in *myo*-inositol chemistry. Various reaction conditions have been investigated under which *myo*-inositol and the derivatives are regioselectively manipulated. To understand the reaction mechanism and regioselectivity of the inositol derivatives, various inositol derivatives have been designed. In particular, the selective functionalization of *myo*-inositol (**1**) has been studied.[1] There have been a few theoretical studies of the conformation of *myo*-inositol.[2] But, owing to the large molecular size, the conformational study resulted in different conclusions depending on the levels of theoretical method used.

Cyclic acetals such as cyclohexylidene and isopropylidene have routinely been used as a protecting group in the synthesis of the *myo*-inositol derivatives to differentiate the six hydroxyl groups.[3] The overall patterns of the reactivity for these acetals toward electrophiles are very similar.[1] Therefore, it is reasonable to think that the bulky acetal groups do not affect the reactivities significantly. In the course of overall selective functionalization, 1,2:4,5-di-*O*-isopropylidene-*myo*-inositol (**2**) and 1,2:4,5-di-*O*-cyclohexylidene-*myo*-inositol (**3**) have been widely used.[4−7] The protecting groups in **2** and **3** impose a ring strain on the central cyclohexyl moiety, which makes it possible to differentiate the remaining two hydroxyl groups. In the experiments, the derivatization in the O3 position turns out to be the major product regardless of the base, electrophiles, and solvents used in the subsequent selective functionalization. Therefore, the selective functionalization seems to have resulted not from the environmental effect but from the compound itself. In spite of some proposed explanations,[5,6] the complexity of the molecules makes it difficult to understand the origin of the selectivity (Figure 1).

Chung and Ryu[6] have recently studied the selectivity of various derivatives of *myo*-inositol. In particular, they studied

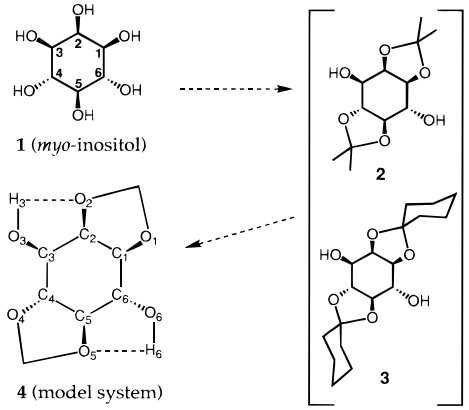

Figure 1. *myo*-Inositol (**1**), its protected species (**2**, **3**), and model system (**4**).

1,2:4,5-di-*O*-isopropylidene-*myo*-inositol, which could be regioselectively functionalized in reactions including alkylation, acylation, and silylation at O3 in preference to O6. Since the selectivity does not depend much on the size of cyclic ketals and the system is large, we devised the simplified model **4** to make our calculation more accurate and efficient. As preliminary work before uncovering the origin of the selectivity, we studied the conformational stability by performing *ab initio* calculations of **4**. The results are compared with the X-ray structure of **3**, in which the intermolecular hydrogen bonds form instead of intramolecular ones.[7] The intermolecular hydrogen bonding would come from the crystal packing effect. In solution, the packing effect is absent, so that the intramolecular hydrogen bonding will be allowed, in particular, in nonpolar and weakly polar solvents. Since in experiment the selectivity of the molecule did not seriously depend on the type of solvent used, the intramolecular hydrogen bonding is likely to be important in solution as well as in the gas state. Indeed, the presence of intramolecular hydrogen bonding was evident in NMR spectra, and the O−H3 group was identified as a proton donor for hydrogen bonding. Since there are two hyroxyl groups in the molecule and each of them can make hydrogen

[⊗] Abstract published in *Advance ACS Abstracts,* May 15, 1996.

S0022-3654(96)00379-6 CCC: $12.00

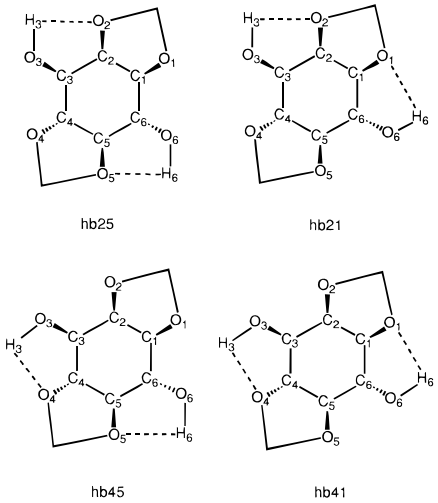

Figure 2. Four conformers of *myo*-inositol. The notation denoted for the four conformers is given as hydrogen-bonded (hb) oxygen numbers.

bonding with one of two neighboring O atoms, there can be four different conformers depending on the orientation of the two −OH groups. The four conformers are denoted with the two numbers of oxygen atoms which are hydrogen bonded by the two −OH groups: (1) hb25, (2) hb21, (3) hb45, and (4) hb41, where "hb" means hydrogen bonding. Here, we report the structures, relative energies, and spectra of the four conformers, comparing with the X-ray structure and NMR and IR spectra (Figure 2).

II. Calculation Method

As mentioned earlier, functionally unimportant isopropylene or cyclohexylene groups in *myo*-inositol were replaced by smaller methylene groups (Figure 1), because this substitution would not greatly affect the calculational results. With these model systems in Figure 2, we performed *ab initio* calculations at various levels of theory: Hartree−Fock (HF) theory, Möller−Plesset second-order perturbation (MP2) theory, density functional theory (DFT), and self-consistent reaction field (SCRF) theory. The basis sets tested here were STO-3G, 3-21G, 6-31G, 6-31G*, and 6-31+G*. In general, it is known that the conformational study dealing with the relative energies of internally hydrogen-bonded structures requires high levels of theory.[8] Since the conformation of *myo*-inositol is related to the internal hydrogen bonding, we examined the consistency between different calculational methods and between different basis sets. Fortunately, all the methods employed here show the consistency for the relative conformational stability. In addition, for a few test cases, the results based on the 6-31+G* basis set are very similar to those based on the 6-31G* basis set. Therefore, all the results discussed here will be based on the 6-31G* basis set unless otherwise specified, in order to give a consistent comparison between various levels of theory. In the case of the DFT method, we used B3-LYP functional, which is known to be one of the most accurate functionals.[9] All the geometries were fully optimized using a GAUSSIAN 92 suite.[10] The four local minima were confirmed by harmonic frequency analyses based on the HF theory, which also provided zero-point vibration energies (ZPVE) and relative free energies at 298 K and 1 atm (G_T^{rel}).[11] In addition, the HF/SCRF calculations were performed in consideration of the solvent effect.

III. Results and Discussion

First, we compared the four conformers predicted by HF, MP2, and DFT methods with the X-ray structure. Table 1 shows the results based on the 6-31G* basis set. Compared with the X-ray structure, the HF results show that the bond lengths between ring carbons and vicinal oxygens are too short (by ∼0.03 Å), while those between ring carbons are similar to the X-ray bond lengths. In the case of the DFT/B3-LYP method, the bond lengths between ring carbons are too long (by ∼0.03 Å), while those between ring carbons and vicinal oxygens are slightly long (by ∼0.01 Å). In this respect, the DFT functional may not be accurate enough to predict the correct bond lengths for this molecular system. A somewhat larger basis set such as 6-31+G* did not improve such errors in both HF and DFT calculations. On the other hand, the MP2 results using the 6-31G* basis set are in good agreement with all the experimental bond lengths within 0.015 Å. As to the 12 bond lengths of C−C in the ring and C−O of the ring carbons and vicinal oxygens, the standard deviations of the MP2/6-31G*-predicted values for hb25, hb21, hb45, and hb41 from the X-ray data are 0.009, 0.011, 0.007, and 0.007 Å, respectively. When the distances between oxygens, which are not the bond lengths, are included, the standard deviations for the 18 distance parameters of hb25, hb21, hb45, and hb41 are 0.026, 0.019, 0.026, and 0.019 Å, respectively. In particular, when the distances and angles for hydrogen bonding are considered, the agreement of conformer hb41 with the X-ray structure is notable. Before discussing more details of the four conformer structures, we compare their relative energies.

As shown in Table 2, hb25 is the lowest energy conformer, followed by hb21. Conformers hb45 and hb41 are slightly higher in energy than conformers hb25 and hb21. The HF/6-31G*-predicted relative energies of hb21, hb45, and hb41 with respect to hb25 are 0.85, 1.63, and 1.93 kcal/mol, respectively. The corresponding MP2/6-31G*-predicted relative energies are 0.80, 1.86, and 1.92 kcal/mol, respectively. These relative energies do not change significantly even in DFT/B3-LYP calculations. We further investigated the zero-point vibrational energy (ZPVE) and thermal energy in the molecule, using the HF calculations. But, these corrections were within 0.2 kcal/mol, as shown in Table 2. Therefore, further calculations using higher levels of theory were not pursued for the thermal energy correction.

Since hb25 is found to be the lowest energy conformer at all levels of theory used here, we investigated the basis set effect for hb25. Table 3 reports the structure of conformer hb25 predicted by HF calculations using different basis sets of STO-3G, 3-21G, 6-31G*, and 6-31+G*. All these results reproduce the X-ray data reasonably well. For hb25, the structural parameters by HF/6-31+G* are very close to those by HF/6-31G* in Table 1. The same was also noted for hb41. As shown in the footnote of Table 2, hb41 is higher in energy than hb25 by 1.81 kcal/mol, similar to 1.93 kcal/mol for HF/6-31G*. Therefore, it is expected that the MP2/6-31+G* results would be similar to the MP2/6-31G* ones; that is, our conclusion would be consistent for very large basis sets.

The conformational stability can be understood in terms of molecular structure, in particular, the hydrogen bond distance. The discussion will be based on the MP2/6-31G* results, unless otherwise specified. For hb25, the bond distance of O2···H3 is particularly short (2.19 Å), which stabilizes the molecule highly by inducing strong intramolecular hydrogen bonding. For hb21, the bond distance of O2···H3 is also short (2.23 Å), stabilizing the molecule highly. The bond distance of O5···H6 is 2.60 Å for hb25, while that of O1···H6 is 2.70 Å for hb21. This leads hb25 to be slightly more stable than hb21. For hb45, two intramolecular hydrogen bond distances of O4···H3 and O5···H6 are ∼2.65 Å, and for hb41, those of O4···H3

TABLE 1: Structures of Four Inositol Conformers in the Gas Phase[a]

		MP2/6-31G*				DFT/6-31G*		HF/6-31G*			
atoms	X-ray[b]	hb25	hb21	hb45	hb41	hb25	hb41	hb25	hb21	hb45	hb41
					Distances between Ring Carbons						
C1−C2	1.531	1.535	1.528	1.541	1.533	1.560	1.561	1.541	1.535	1.545	1.539
C2−C3	1.530	1.534	1.531	1.525	1.523	1.561	1.547	1.537	1.535	1.530	1.528
C3−C4	1.500	1.509	1.510	1.504	1.504	1.533	1.527	1.511	1.511	1.507	1.507
C4−C5	1.497	1.508	1.515	1.504	1.511	1.531	1.534	1.508	1.514	1.505	1.510
C5−C6	1.498	1.503	1.501	1.503	1.500	1.526	1.521	1.506	1.505	1.507	1.505
C6−C1	1.546	1.533	1.537	1.537	1.542	1.561	1.574	1.538	1.541	1.541	1.545
					Distances between Ring Carbon and Vicinal Oxygen						
C1−O1	1.439	1.431	1.438	1.429	1.435	1.445	1.449	1.406	1.411	1.404	1.409
C2−O2	1.426	1.441	1.441	1.432	1.433	1.456	1.448	1.412	1.412	1.404	1.405
C3−O3	1.419	1.416	1.417	1.417	1.417	1.429	1.431	1.391	1.391	1.392	1.392
C4−O4	1.439	1.426	1.423	1.430	1.428	1.441	1.442	1.400	1.398	1.405	1.403
C5−O5	1.436	1.427	1.422	1.429	1.425	1.442	1.441	1.401	1.397	1.403	1.399
C6−O6	1.422	1.421	1.419	1.422	1.419	1.435	1.432	1.396	1.395	1.397	1.396
					Distances between Oxygens						
O1−O2	2.286	2.300	2.300	2.300	2.303	2.323	2.236	2.244	2.245	2.245	2.247
O2−O3	2.746	2.710	2.734	2.752	2.774	2.740	2.809	2.709	2.727	2.746	2.763
O3−O4	3.003	3.085	3.057	3.049	3.017	3.113	3.048	3.053	3.034	3.028	3.006
O4−O5	2.310	2.321	2.322	2.324	2.323	2.348	2.348	2.267	2.266	2.268	2.267
O5−O6	2.948	2.977	2.949	3.017	2.984	3.036	3.030	2.980	2.947	3.009	2.973
O6−O1	3.079	3.040	3.045	3.020	3.026	3.090	3.083	3.024	3.045	3.012	3.031
					Distances of O−H Bonds						
O3−H3	0.820	0.976	0.976	0.975	0.975	0.983	0.982	0.950	0.950	0.949	0.949
O6−H6	0.860	0.975	0.975	0.975	0.976	0.982	0.982	0.949	0.949	0.949	0.949
					Distances for Hydrogen Bonding						
O2−H3	3.495	2.189	2.231	3.611	3.627	2.213	3.676	2.255	2.291	3.608	3.620
O4−H3	3.172	3.537	3.495	2.677	2.624	3.568	2.640	3.494	3.456	2.706	2.668
O1−H6	3.051	3.901	2.700	3.860	2.669	3.950	2.724	3.849	2.788	3.822	2.761
O5−H6	3.591	2.598	3.826	2.674	3.861	2.665	3.908	2.680	3.790	2.736	3.817
					Angles for Hydrogen Bonding or Complexation						
O2−H3−O3	21.1	112.0	110.8	24.4	25.1	112.2	24.1	108.4	107.2	21.5	22.1
O4−H3−O3	70.7	55.1	55.9	103.0	104.3	55.1	105.2	55.2	56.3	100.6	101.5
O1−H6−O6	83.8	24.5	101.2	26.6	102.0	25.2	102.0	25.9	96.5	27.4	97.3
O5−H6−O6	36.9	103.2	22.5	101.1	22.7	102.7	23.1	99.0	23.9	97.4	23.7
					Angles between Ring Carbons						
C1−C2−C3	117.9	120.4	119.0	117.9	116.3	120.1	116.2	119.9	118.8	117.7	116.6
C2−C3−C4	107.0	106.9	107.4	106.7	107.2	107.4	107.7	107.4	107.7	107.1	107.4
C3−C4−C5	110.5	109.6	111.1	109.3	110.8	109.8	110.9	109.8	111.0	109.6	110.9
C4−C5−C6	110.0	111.8	110.3	111.5	109.7	111.7	109.6	111.7	110.6	111.4	110.1
C5−C6−C1	107.4	106.6	106.7	107.1	106.9	107.2	107.3	107.1	107.0	107.3	107.2
C6−C1−C2	115.3	114.4	115.3	114.5	115.4	115.6	116.5	115.4	116.2	115.5	116.2
					Angles between Ring Carbons and Vicinal Oxygens						
C6−C1−O1	110.1	111.9	109.7	110.9	109.1	112.3	109.3	111.3	110.0	110.8	109.5
C1−C2−O2	101.6	100.2	100.0	100.0	99.9	101.1	100.7	100.6	100.6	100.4	100.3
C2−C3−O3	110.5	110.2	110.2	108.2	108.4	110.5	108.7	110.4	110.5	108.8	108.9
C3−C4−O4	114.6	115.3	114.5	114.4	113.7	115.6	114.2	116.4	115.8	115.7	115.1
C4−C5−O5	101.2	102.3	101.4	101.7	100.9	102.4	101.2	101.7	101.1	101.4	100.8
C5−C6−O6	109.0	112.6	110.4	112.6	110.5	113.0	110.6	112.7	110.5	112.6	110.5
					Torsional Angles between Ring Carbons						
C1−C2−C3−C4	42.3	40.5	40.0	46.0	45.4	38.2	43.4	39.2	39.1	44.3	43.9
C2−C3−C4−C5	−58.4	−55.1	−54.9	−59.4	−59.3	−55.4	−59.6	−55.7	−55.6	−59.4	−59.3
C3−C4−C5−C6	72.6	72.4	71.2	72.0	71.3	72.8	71.8	72.5	71.6	72.2	71.5
C4−C5−C6−C1	−60.1	−62.7	−62.3	−60.5	−60.7	−61.2	−59.6	−61.3	−60.9	−59.6	−59.5
C5−C6−C1−C2	42.8	43.4	45.8	44.0	47.0	40.5	44.4	41.3	43.3	42.4	44.5
C6−C1−C2−C3	−36.9	−36.3	−37.6	−40.2	−41.8	−32.3	−38.2	−33.8	−35.1	−37.8	−39.1
					Torsional Angles between Ring Carbons and Vicinal Oxygens						
C5−C6−C1−O1	21.5	22.0	19.4	21.9	18.8	23.3	20.0	24.0	22.0	23.6	21.4
C6−C1−C2−O2	82.6	79.3	78.7	78.1	77.0	84.6	82.2	84.5	83.7	85.5	81.7
C1−C2−C3−O3	15.0	14.2	14.4	10.6	11.1	15.6	12.4	15.1	15.1	11.7	12.1
C2−C3−C4−O4	−7.7	−12.0	−11.3	−7.8	−6.8	−10.7	−5.8	−10.6	−10.0	−7.2	−6.6
C3−C4−C5−O5	−14.8	−14.9	−13.9	−14.8	−14.4	−15.6	−15.5	−16.0	−15.4	−16.1	−15.7
C4−C5−C6−O6	0.3	0.1	2.1	−2.1	0.6	−1.3	−0.1	−0.6	1.1	−2.3	−0.2
					Torsional Angles between Free Hydroxyl Groups and Adjacent Methine Groups						
H3−O3−C3−H	10.3	−13.5	−11.9	66.8	68.4	−14.4	69.3	−12.9	−11.2	65.9	67.2
H6−O6−C6−H	−36.7	65.4	−59.6	62.2	−60.3	64.5	−59.6	61.5	−55.2	58.9	−56.1

[a] Distances are in Å, angles in deg. [b] Reference 6.

and O1···H6 are also ∼2.65 Å. These correspond to weak intramolecular hydrogen bonds to stabilize the molecules slightly. Therefore, hb25 is the most stable, followed by hb21, and then hb45 and hb41.

TABLE 2: Energies of the Four Conformers Based on the 6-31G* Basis Set[a]

	HF					HF/SCRF[b]		MP2		DFT	
	E	E^{rel}	E_0^{rel}	H_T^{rel}	G_T^{rel}	*E*	E^{rel}	*E*	E^{rel}	*E*	E^{rel}
hb25	−759.044 91	0.00	0.00	0.00	0.00	−759.450 60	0.00	−761.139 17	0.00	−763.088 10	0.00
hb21	−759.043 56	0.85	0.81	0.81	0.88			−761.137 90	0.80		
hb45	−759.042 32	1.63	1.48	1.51	1.55			−761.136 21	1.86		
hb41	−759.041 84	1.93	1.82	1.82	1.96	−759.041 91	1.98	−761.136 11	1.92	−763.085 06	1.91

[a] E_0^{rel} is the internal energy with zero point energy correction at 0 K; H_T^{rel} and G_T^{rel} are the enthalpies and Gibbs free energies at $T = 298$ K and 1 atm. Energies (*E*) are in hartrees; all relative energies (E^{rel}) are in kcal/mol. [b] Dielectric constant: $\epsilon = 20$. The HF energies using the 6-31+G* basis set are as follows: *E*(hb25) = −759.068 29 hartrees, *E*(hb41) = −759.06542 hartrees; E^{rel}(hb25) = 0, E^{rel}(hb41) = 1.81 kcal/mol.

TABLE 3: HF Structures of the Lowest Energy Conformers (hb25) Predicted by Various Basis Sets[a]

atoms	STO-3G	3-21G	6-31G	6-31+G*
Distances between Ring Carbons				
C1−C2	1.569	1.544	1.547	1.543
C2−C3	1.567	1.536	1.536	1.537
C3−C4	1.549	1.506	1.507	1.512
C4−C5	1.539	1.512	1.514	1.510
C5−C6	1.547	1.498	1.501	1.507
C6−C1	1.570	1.532	1.533	1.538
Distances between Ring Carbon and Vicinal Oxygen				
C1−O1	1.446	1.450	1.442	1.407
C2−O2	1.440	1.458	1.451	1.411
C3−O3	1.430	1.426	1.416	1.392
C4−O4	1.438	1.444	1.435	1.401
C5−O5	1.438	1.444	1.434	1.402
C6−O6	1.433	1.433	1.423	1.398

[a] Distances are in Å.

Taking into account the solvent effect with dielectric constant of 20 (since the dielectric constants of the experimental solutions such as CH_2Cl, toluene, pyridine, and DMF range from ∼10 to ∼40),[6] the relative energies of the four conformers predicted by HF/SCRF are very similar to those predicted by the HF energies in the gas phase (i.e., with the dielectric constant of 1). For this reason, it is expected that the MP2/SCRF relative energies of the four conformers may not be significantly different from the MP2 results. Therefore, all the levels of theory used here lead to a consistent conclusion: the lowest energy conformer is hb25, while hb41 is the highest in energy among the four conformers.

Now, we go back to the structural comparison between the calculated and X-ray geometries. As shown in Table 1, among the four conformers, the geometrical structure of hb41 is the closest to the X-ray structure, though hb25 gives the lowest energy. The similarities and differences between the structures of the X-ray, hb41, and hb25 can be distinctively noted from the hydrogen bond distances of O2···H3, O1···H6, O5···H6, and O4···H3 and hydrogen bond angles of O2···H3−O3, O4···H3−O3, O1···H6−O6, and O5···H6−O6, as shown in Table 1. The X-ray structure reflects some of conformer hb41, which has the weakest intramolecular hydrogen bonding so that the intermolecular hydrogen bonding would be easier than other conformers. In this regard, it is reasonable that though hb41 is slightly higher in energy than other conformers, the X-ray structure is more similar to hb41 than other conformers. Indeed, intermolecular hydrogen bonds were found in the X-ray structure, while intramolecular hydrogen bonds were present in the NMR experiment.[6] The distances of O2···H3 and O5···H6 in the X-ray data are respectively 3.5 and 3.6 Å, while the corresponding distances in hb25 are 2.2 and 2.6 Å, respectively. This indicates that the intramolecular hydrogen bonds form in hb25, while this hydrogen bonding conformation changes in the crystalized structure. It is known that the hydrogen conformation in a crystal is often quite different from that in the gas phase.[12]

Structure hb25 is in good agreement with the NMR experiment, in which H3 is oriented toward O2 instead of O4, while the orientation of H6 toward O5 (instead of O1) is less clearly shown. The ^{1}H NMR spectra at 300 MHz in deuteriochloroform revealed two hydroxyl peaks at $\delta = 2.36$ (d, *J* 8.8 Hz for H3) and $\delta = 2.45$ (d, *J* 2.9 Hz for H6), from which the coupling constants between the hydroxyl protons and the ring methine protons at C3 and C6 could be roughly correlated to dihedral angles of ∼150° and ∼60° (or ∼110°), respectively.[6] The torsional angles of H3−O3−C3−H and H6−O6−C6−H are [166°,65°] for hb25, [168°,120°] for hb21, [67°,62°] for hb45, and [68°,120°] for hb41 (Table 1). Therefore, the torsional angles predicted by hb25 and hb21 give the best agreements with the torsional angles roughly estimated from the NMR data. Since hb25 is found to be energetically the most stable, it is expected that the structure of hb25 is similar to that in solution. On the other hand, structure hb41 seems to be somewhat similar to the X-ray structure, since hb41 has the weakest intramolecular hydrogen bonding among the four conformers.

Table 4 shows the O−H stretching vibrational frequencies for the four conformers. Since in hb25 the intramolecular hydrogen bond distance of O2···H3 (2.2 Å) is shorter than that of O5···H6 (2.6 Å), there should appear a frequency difference between the two OH stretching modes. If the hydrogen bond angle is 180° (linear), there occurs a large frequency shift (∼100 cm^{-1} red shift) due to direct coupling between O−H and H···O stretching modes. However, in this system the intramolecular hydrogen bond angles (101−112°) are near 90°, so that the frequency shifts would arise almost from the indirect coupling (i.e., the second-order perturbation effect). Thus, the frequency shifts should be small. Indeed, Table 4 shows small red shifts (∼5 cm^{-1}) for hb25 and hb21 (which have highly bent bond angles of ∼110° in spite of short hydrogen bond distances of ∼2.2 Å) and negligible red shifts (only ∼1 cm^{-1}) for hb41 and hb45 (which have almost perpendicular bond angles of ∼100°

TABLE 4: HF/6-31G* Vibrational Frequencies (ω) and Infrared/Raman Intensities (IR/rm) of the O−H Stretching Modes of the Four Conformers in the Gas Phase[a]

	ω[scaled] (IR/rm)			
stretching modes	hb25	hb21	hb45	hb41
O6−H6	4079[3643](69/78)	4080[3643](65/84)	4082[3645](67/82)	4079[3643](48/102)
O3−H3	4074[3638](67/34)	4074[3638](62/34)	4079[3643](70/77)	4078[3642](89/57)

[a] Frequencies are in cm^{-1}; IR and Raman intensities are in km/mol and $Å^4$/amu, respectively. Scaled frequencies were scaled by a factor of 0.893 in order to predict realistic frequencies (ref 10).

at normal hydrogen bond distances of ∼2.7 Å). Even if the molecule interacts with the solvent molecules of CH_2Cl_2, the frequency shift would not be large, but the dimer formation would have a large frequency shift, since the frequency shift of the hydrogen-bonded O−H stretching from the free O−H stretching is highly influenced by geometric factors such as distance and angle of hydrogen bond as well as hydrogen bond strength. Indeed, Kuhn[13] found from IR spectra of various cyclic diols that the splitting of O−H frequencies due to intramolecular hydrogen bonding ranged from 0 to 70 cm^{-1}, while the splitting due to intermolecular hydrogen bonding ranged from 50 to 200 cm^{-1}. As a simple model study, we compared the hydrogen bond interaction between methanol and CH_2Cl with that in the methanol dimer, using HF/6-31G* calculations. The former gives only 7 cm^{-1} red shift, while the latter gives 60 cm^{-1} red shift. The experimental IR spectra of 1,2:4,5-di-*O*-isopropylidene-*myo*-inositol showed two broad peaks around 3500 cm^{-1}: 3585 and 3475 cm^{-1}, in which the latter peak appeared only at very high concentrations. The HF/6-31G* harmonic vibrational frequencies of the O−H bonds are predicted to be ∼4080 cm^{-1} (Table 4). Since the HF/6-31G* harmonic frequencies are, in general, required to be scaled down by a factor of ∼0.893 in order to predict realistic frequencies,[10] this scaling gives ∼3640 cm^{-1} for the O−H bonds. In deuteriochloroform solution (of dielectric constant ∼9), the O−H stretching frequencies of the inositol monomer are likely to red shift to the experimental peak of 3585 cm^{-1}. The peak of 3475 cm^{-1} is considered to be the O−H frequencies of the inositol dimers due to the following reason. The dimer is likely to have two intermolecular hydrogen bonds between two monomers by the interactions of O−H3 and O2 in one monomer with, respectively, O2 and O−H3 (or O5 and O−H6) in the other monomer, or by the interactions of O−H6 and O5 in one monomer with, respectively, O5 and O−H6 (or O2 and O−H3) in the other monomer. Therefore, the strong binding by two additive hydrogen bonds would enhance the frequency shifts very highly. That is, a large frequency splitting (110 cm^{-1}) of the O−H frequencies is expected in concentrate solutions of inositol, based on our results.

IV. Conclusion

Four levels of *ab initio* theory (i.e., HF, MP2, DFT, and SCRF) combined with various basis sets gave a consistent result that among four conformers of the *myo*-inositol, hb25 gives the lowest energy, followed by hb21, hb45, and hb41. Conformer hb25 has strong intramolecular hydrogen bonding. Thermal energy corrections were negligible for this system. In the reaction field with the dielectric constant of 20, the relative energies of the four conformers did not change significantly. Therefore, even in solution, hb25 is expected to be the most stable conformer with strong intramolecular hydrogen bonding. This is in agreement with the NMR experiment. The frequency splitting between the two OH vibrational frequencies due to the difference in hydrogen bond distance and angle as well as in strength of the intramolecular hydrogen bonding is found to be very small (only 1−6 cm^{-1}) in contrast to a large frequency difference (∼100 cm^{-1}) to appear in the intermolecular hydrogen bonding in solutions of high concentration and in crystals. Structure hb41 which has weak intramolecular hydrogen bonding is found to be in better agreement with the X-ray structure than structure hb25. This seems to be related with the possibility that structure hb41 can have better intermolecular hydrogen bonding due to weak intramolecular hydrogen bonding, because intermolecular hydrogen bonding is important for crystal packing.

Acknowledgment. This work was supported by KOSEF/CBM and the Ministry of Education/(BSRI-95-3436 and BSRI-95-3437).

References and Notes

(1) (a) Angyal, S. J.; Tate, M. E.; Gero, S. D. *J. Chem. Soc.* **1961**, 4416. (b) Gigg, R.; Warren, C. D. *J. Chem. Soc.* **1961**, 4116. (c) Kiely, D. E.; Abruscato, G. J.; Baburao, V. *Carbohydr. Res.* **1974**, *34*, 307. (d) Watanabe, Y.; Ogasawara, T.; Nakahira, H.; Masuki, T.; Oazki, S. *Tetrahedron Lett.* **1988**, *29*, 5259. (e) Gigg, J.; Gigg, R.; Payne, S.; Conant, R. *Carbohydrate Res.* **1985**, *142*, 132. (f) Reese, C. B.; Ward, J. G. *Tetrahedron Lett.* **1987**, *28*, 2309. (g) Lee, H. W.; Kishi, Y. *J. Org. Chem.* **1985**, *50*, 4402. (h) Billinton, D. C.; Baker, R. *J. Chem. Soc., Chem. Commun.* **1987**, 1011. (i) Billinton, D. C.; Baker, R.; Kulagowski, J. J.; Mawer, I. M.; Vacca, J. P.; de Solms, S. J.; Huff, J. R. *J. Chem. Soc., Perkin Trans.* **1987**, *1*, 1423.

(2) Liang, C.; Ewig, C. S.; Stouch, T. R.; Hagler, A. T. *J. Am. Chem. Soc.* **1994**, *16*, 3904.

(3) (a) Watanabe, Y.; Mitani, M.; Morita, T.; Ozaki, S. *J. Chem. Soc., Chem. Commun.* **1989**, 482. (b) Zapata, A.; Fernandez de la Pradilla, R.; Martin-Lomas, M.; Penades, S. *J. Org. Chem.* **1991**, *56*, 444. (c) Gilbert, I. H.; Holmes, A. B.; Young, R. C. *Tetrahedron Lett.* **1990**, *31*, 2633.

(4) (a) Greene, T. W.; Wuts, P. G. M. *Protective Groups in Organic Synthesis*; Wiley: New York, 1991. (b) Garegg, P. J.; Iversen, T.; Johansson, R.; Lindberg, B. *Carbohydr. Res.* **1984**, *130*, 322. (c) Yu, K.-L.; Frazer-Reid, B. *Tetrahedron Lett.* **1988**, *29*, 979. (d) Billington, D. C.; Baker, R.; Kulagowski, J. J.; Mawer, I. M. *J. Chem. Soc., Chem. Commun.* **1987**, 314. (e) Moltkovesky, J. G.; Bergelson, L. D. *Tetrahedron Lett.* **1971**, 4791. (f) Nagashima, N.; Ohno, N. *Chem. Lett.* **1987**, 141. (g) Billington, D. C.; Baker, R. *J. Chem. Soc., Chem. Commun.* **1987**, 1011. (h) Stepanov, A. E.; Tuorskaya, O. O.; Klyaschitskii, B. A.; Shvets, V. I.; Evstingneeva, R. P. *Zh. Obshch. Chim.* **1972**, *42*, 709. (i) Kozlova, S. P.; Pekarskaya, I. S.; Klyaschitskii, B. A.; Shvets, V. I.; Evstigneeva, R. P.; *Zh. Obshch. Chim.* **1972**, *42*, 702. (j) Klyaschitskii, B. A.; Pimenova, V. V.; Bashkatova, A. I.; Zhelvakova, E. G.; Sokolov, S. D.; Shvets, V. I.; Evistingneeva, R. P.; *Zh. Obshch. Chim.* **1970**, *40*, 2482. (k) Stepanov, A. E.; Shvets, V. I.; *Chem. Phys. Lipids.* **1979**, *25*, 247.

(5) Vernon, G. S. *Heterocycles* **1982**, *19*, 1939.

(6) Chung, S.-K.; Ryu, Y. *Carbohydr. Res.* **1994**, *258*, 145.

(7) Chung, S.-K.; Ryu, Y.; Chang, Y.-T.; Whang, D.; Kim, K. *Carbohydr. Res.* **1994**, *253*, 13.

(8) (a) Oie, T.; Topol, I. A.; Burt, *J. Phys. Chem.* **1994**, *98*, 1121. (b) Lee, S. J.; Mhin, B. J.; Cho, S. J.; Lee, J. Y.; Kim, K. S. *J. Phys. Chem.* **1994**, *98*, 1129.

(9) (a) Becke, A. D. *J. Chem. Phys.* **1993**, *98*, 5648. (b) Kim, K.; Jordan, K. D. *J. Phys. Chem.* **1994**, *98*, 10089. (c) Lee, C.; Yang, W.; Parr, R. G. *Phys. Rev. B* **1993**, *37*, 785.

(10) *Gaussian*; Frisch, M. J.; Trucks, G. W.; Head-Gordon, M.; Gill, P. M. W.; Wong, J. B. F.; Johnson, B. G.; Schlegel, H. B.; Robb, M. A.; Replogle, E. S.; Gomperts, R.; Andres, J. A.; Raghavachari, K.; Binkley, J. S.; Gonzalez, C.; Martin, R. L.; Fox, D. J.; Defrees, D. J.; Baker, J.; Stewart, J. J. P.; Pople, J. A. Gaussian Inc.: Pittsburgh, 1992.

(11) Kim, K. S.; Mhin, B. J.; Choi, U.-S.; Lee, K. *J. Chem. Phys.* **1992**, *97*, 6649.

(12) (a) Steiner, T.; Saenger, W. *Acta Crystallogr.* **1992**, *B48*, 819. (b) Kouwijzer, M. L. C. E.; van Eijck, B. P.; Kroes, S. J.; Kroon, J. *J. Comput. Chem.* **1993**, *14*, 1281.

(13) Kuhn, L. P. *J. Am. Chem. Soc.* **1952**, *74*, 2492; **1954**, *76*, 4323.

JP9603795